JOURNAL OF MATERIALS SCIENCE 8 (1973) 1253–1270

High temperature creep of lithium zinc silicate glass-ceramics

Part 1 *General behaviour and creep mechanisms*

R. MORRELL*, K. H. G. ASHBEE
H. H. Wills Physics Laboratory, University of Bristol, UK

Two compositionally similar but morphologically different glass-ceramics containing about 20% residual glass phase have been creep-tested in tension and compression between 600 and 800°C. High stresses cause low strain failure in both materials but at low stresses there is considerable plasticity, strains greater than 30% being produced in one material. At the same stress and temperature, creep in tension is much faster than in compression, the ratio of secondary creep rates varying from 10 to 1000. The activation energy for secondary creep, 600 ± 60 kJ mol^{-1}, is effectively independent of stress, and within the scatter of the data is the same in tension and compression for both materials. The stress exponent is independent of temperature, but strongly dependent on stress, varying between 1.0 to 6.0 for the two glass-ceramics over the stress ranges used. This behaviour is similar to that exhibited by basic refractories, and is attributed to voids created within the glassy material between the crystals. The higher the stress, the easier it is to create the voids which are responsible for enhanced creep rates and low failure strain. A simple model is described to illustrate this mechanism.

1. Introduction

Glass-ceramics are a relatively recent and important development in the ceramics field, and have been shown by many authors to possess such useful properties as high mechanical and dielectric strengths, negligible porosity and good thermal shock resistance (see McMillan [1]). However, relatively little has been published on the strength above room temperature, and even less on the nature of plastic deformation in these materials. If glass-ceramics are to be developed for use at elevated temperatures some knowledge of the plasticity and strength limiting factors is important.

Lyall [2] investigated the strength of some Li_2O-ZnO-SiO_2 glass-ceramics, and showed that the room temperature strength is retained up to temperatures at which bulk plasticity is detected. At higher temperatures very rapid flow is obtained at low stresses, and, since the microstructure appears to be unchanged by plastic deformation, it was concluded that strain is accommodated by flow of the residual glass phase, estimated to occupy about 20% of the total volume. However, in stress relaxation tests, Lyall found that very long times are required for the stress to relax to zero and suggested that the crystalline material is multiply-connected and therefore also obliged to deform. To accommodate bulk plasticity without change of microstructure, it was necessary to postulate that the links between crystals can be severed and recreated.

In an attempt to interpret the plasticity of glass-ceramics containing a large proportion of residual glass, the present paper reports the results of an extensive investigation into the creep behaviour of two Li_2O-ZnO-SiO_2 glass-ceramics. Although these particular materials are not intended for high temperature use the results obtained should be relevant to other types of glass bonded ceramics including porcelains, aluminas and dense firebrick.

*Now at National Physical Laboratory, Division of Inorganic and Metallic Structure, Teddington, Middlesex.

TABLE I Raw materials and composition of glasses (i) and (ii)

Raw materials	Glass (i) (wt %)		Glass (ii) (wt %)	
SiO_2	58.50		59.40	
Li_2CO_3	25.19		25.57	
ZnO	6.55		8.33	
$Zn_3(PO_4)_2.4H_2O$	5.52		2.36	
KNO_3	4.30		4.36	
Calculated oxide content	(mol %)		(mol %)	
	Total	Major constituents	Total	Major constituents
SiO_2	66.50	68.0	66.83	68.0
Li_2O	23.20	23.8	23.40	23.8
ZnO	7.96	8.15	8.01	8.15
K_2O	1.46	—	1.45	—
P_2O_5	0.84	—	0.33	—

2. The glass-ceramics and their microstructure

2.1. Composition and manufacture

The two glass-ceramics investigated, (i) a fine-grained and (ii) a coarser grained material, were derived from similar glass compositions and differed only in the amount of P_2O_5 nucleating agent added to the mix (Table I). They possessed considerably different microstructures but contained the same crystalline species in approximately the same proportions. The starting materials were precipitated silica, Li_2CO_3, ZnO, $Zn_3(PO_4)_2.4H_2O$ and KNO_3, all of reagent grade supplied by BDH Ltd. The powders were mixed in a ball mill, compacted and melted in a platinum crucible heated by an r.f. coil. After complete melting, the glass was quenched into distilled water, ground in large batches, remixed, and then refined in small quantities for about 4 h at 1250 to 1300°C. Glass rods, with diameter 9.5 mm for tensile testing and 3.7 mm for compression testing, were vacuum cast into preheated graphite moulds, annealed at 480°C and cut to suitable lengths for heat-treatment.

2.2. Heat-treatment

Preliminary creep tests, and the data obtained by Lyall [2] showed that rapid deformation of these materials occurred at very low stresses above 800°C. In order to ensure complete crystallization, a maximum heat-treatment temperature of 850°C was used for all specimens so that further crystallization during creep testing was unlikely. The heating schedule used a constant heating rate of 2°C min^{-1} with holds for 1 h at 500°C and at 850°C, followed by furnace cooling. During this time, the specimens were supported in a bed of compacted precipitated silica to minimize deformation under their own weight.

2.3. Microstructure

Glass (i) produces a glass-ceramic (Fig. 1) which consists of equiaxed crystals of lithium disilicate about 1 μm across with smaller β-lithium zinc silicate crystals [3] between them. This latter phase is deeply etched in Fig. 1b. X-ray powder patterns show that a small amount of β-quartz is also present, although this could not be distinguished in the micrographs. Strong diffuse haloes, indicating the presence of a considerable amount of amorphous material, were also present in the diffraction patterns. The crystals in Fig. 1a appear to be surrounded by a continuous phase, which is presumably a residual glass that did not crystallize during the heat-treatment.

Glass (ii) produces a structurally more complex material (Fig. 2). The lithium disilicate crystals grow in large star-shaped, partially interlocked clusters from a much smaller number of nuclei than glass (i). Smaller crystals of β-lithium zinc silicate and β-quartz then form on and between the clusters. The residual glass occupies the space between the small crystals and exists also in larger volumes of up to 15 μm across between the clusters. X-ray microprobe analysis shows this phase to be potassium rich but depleted in zinc and presumably lithium. Quantitative analysis was not possible since the depths of the glassy areas were not large enough to ensure that no crystalline material was within the electron beam penetration volume.

TABLE II Phase proportions by area analysis

Phase	Average crystal size (μm)		Volume fraction (%)	
	Glass-ceramic (i)	Glass-ceramic (ii)	Glass-ceramic (i)	Glass-ceramic (ii)
Lithium disilicate	1.1 μm	15 μm in clusters up to 40 μm	60 ± 5	55 ± 5
β-lithium zinc silicate	0.2 to 0.7 μm lath-shaped	0.5 to 2.0 μm lath-shaped	18 ± 3	20 ± 3
β-quartz	Not distinguished	1.0 to 2.0 μm	—	5 ± 2
Glass phase	Layers between crystals 0.2 μm thick	Layers between crystals 0.3 μm thick + areas 15 μm across	20 ± 5	20 ± 5

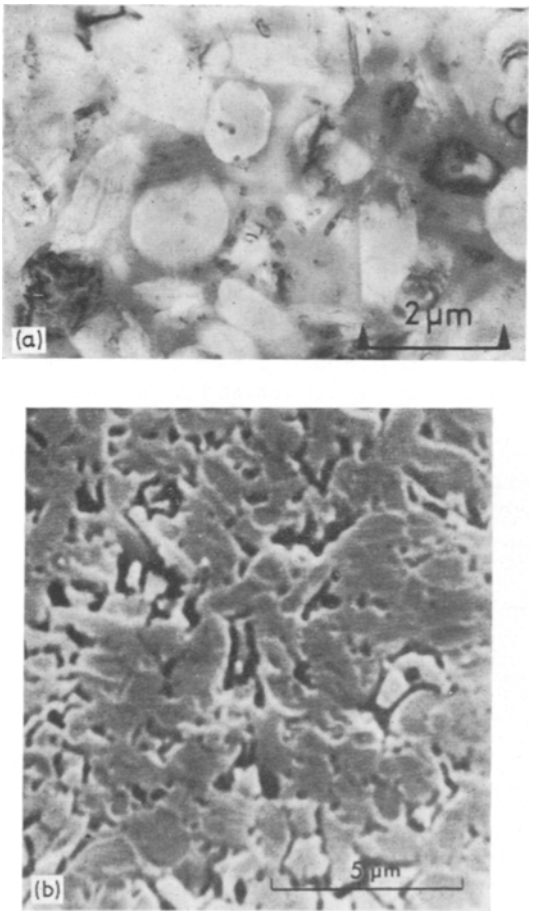

Figure 1 Microstructure of glass-ceramic (i), (a) transmission electron microscopy, (b) etched 10 sec in 2% HF, SEM.

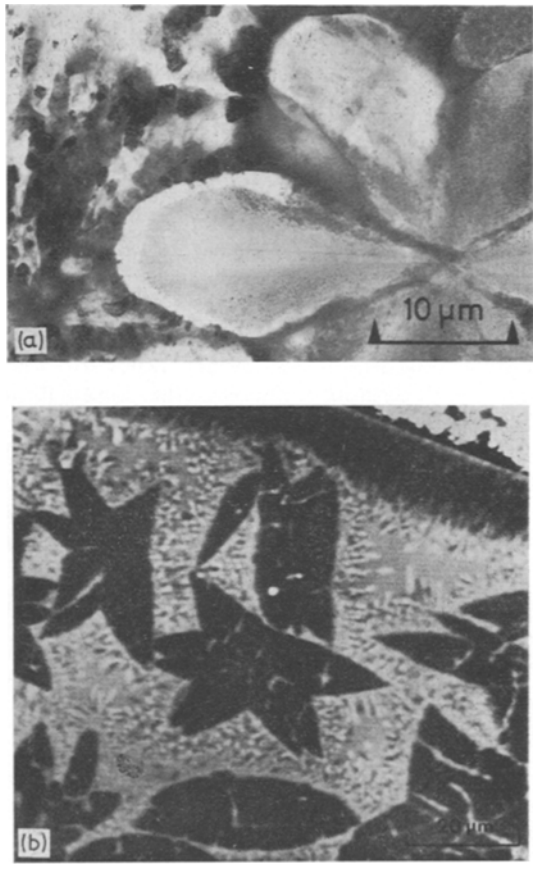

Figure 2 Microstructure of glass-ceramic (ii), (a) transmission electron microscopy, (b) etched 10 sec in 2% HF, SEM.

Since the only difference between the two original glass compositions is the P_2O_5 concentrations, and since in the final glass-ceramic structures the same crystalline phases are present in approximately the same proportions by area analysis (Table II), it is reasonable to suppose that the residual glass phases are of similar composition. This composition, calculated from the area proportions of the phases by assuming that all the Li^+ and Zn^{2+} ions are in the crystal phases and that there were no losses during manufacture, is approximately 88% SiO_2, 12%

K_2O by weight. Ignoring the small amounts of other oxides likely to be present, the residual glass probably has an annealing temperature of about 500°C and a viscosity ranging from 10^7 to 10^2 Ns m^{-2} in the temperature range 600 to 800°C [4].

Both the original glasses and glass-ceramic (i) were pore-free to within an experimental resolution of about 0.2 μm, but glass-ceramic (ii) contained about 0.2% of large closed pores 50 to 100 μm across as a result of rapid bulk volume changes on crystallization. Each glass-ceramic had a layer of surface crystallization, predominantly needles of lithium disilicate, of thickness approximately equal to the bulk lithium disilicate grain diameter.

3. Creep tests

3.1. Apparatus

In order to obtain reproducible creep measurements at failure strains as low as 0.3% a tensile creep apparatus was designed to minimize non-axialities of loading. The basic principles of the apparatus are described elsewhere [5]. The transducer strain measuring system was capable of recording strain-rates in the range 10^{-8} to 10^{-4} sec^{-1} without difficulty, the lower limit being set by the mechanical and thermal stability of the environment and the electrical stability of the strain measuring system.

The compressive creep tests were performed using a "Denison" machine equipped with a compression jig. A small "Kanthal"-wound furnace surrounded the creep specimen which was loaded between ground alumina push rods fixed in collars attached to the compression plattens. An axially mounted displacement transducer monitored the relative movement of the plattens. No creep was detected in the loading system after several thousand hours use. Compression specimens were cut in the form of cylinders of length 7.5 mm from the crystallized rod, and retained their original layer of surface crystallization, unlike the tensile specimens which had a machined gauge-length.

3.2. Testing programme and shape of creep curves

Below 600°C, the resistance to creep of both glass-ceramics is high, and easily measured creep rates required high stresses which produced very low and irreproducible strains to failure. Above 800°C, the materials possess very little strength, and rapid deformation occurs at the low loads required to maintain specimen and load-train alignment. The creep results reported are generally those derived from tests between 600 and 800°C, and at stresses between 0.69 and 13.8 MN m^{-2} in tension and 3.3 and 71.7 MN m^{-2} in compression. Tests at a given stress level were performed within a temperature range which gave strain-rates between 10^{-8} and 10^{-4} sec^{-1}. The different stress ranges in tension and compression reflect that between 3.5 and 7.0

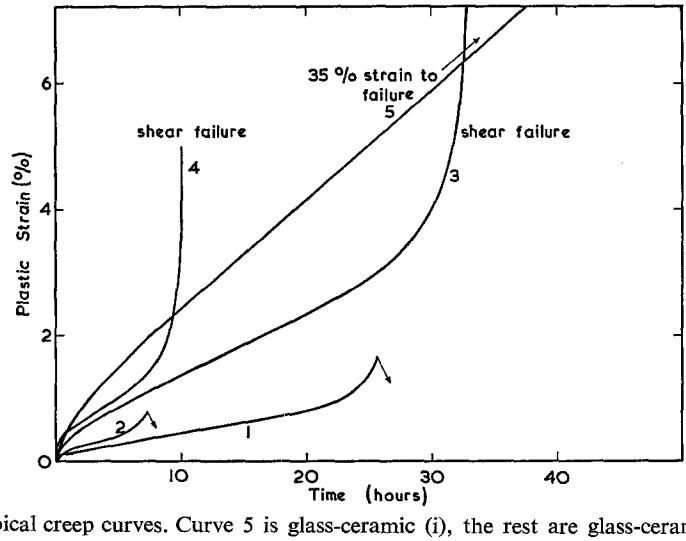

Figure 3 Shapes of typical creep curves. Curve 5 is glass-ceramic (i), the rest are glass-ceramic (ii). Testing conditions: 1. tension, 700°C, 3.45 MN m^{-2}; 2. tension, 636°C, 13.8 MN m^{-2}; 3. compression, 681°C, 26 MN m^{-2}; 4. compression, 659°C, 48.8 MN m^{-2}; 5. tension, 740°C, 0.69 MN m^{-2}.

times the tensile stress is required in compression to maintain the same creep rate, the factor varying with stress differently for each glass-ceramic.

The general shapes of creep curves are similar for the two materials and are shown in Fig. 3. In tension, primary creep is followed by a steady secondary creep (except at high stresses) which contributes up to 80% of the total strain to fracture. Tertiary creep is accompanied by the growth of blunt cracks originating both internally and from the surface. At high stresses, the strain to fracture is very small and distinct secondary creep is not observed, primary and tertiary creep tending to overlap. In these cases, the minimum creep rate was measured and for comparison was plotted along with the true secondary creep rates obtained at lower stresses.

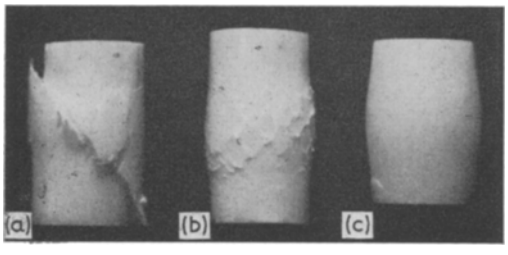

Figure 4 Three modes of compression failure, (a) at high stresses in both glass-ceramics, (b) low stresses in glass-ceramic (ii), and (c) low stresses in glass-ceramic (i).

In compression, primary creep is again followed by a steady secondary creep (a minimum creep rate at the highest stresses used) but tertiary creep is not always observed. Deformation of the specimens occurs in three ways as shown in Fig. 4. At high stresses in both glass-ceramics, failure commences at strains of 1 to 2% resulting in rapid shear of the two halves of the specimens along a plane at between 30 to 40° to the compression axis (Fig. 4a), with voidage being produced in the narrow shear zone. At low stresses in glass-ceramic (ii) (Fig. 4b) considerable voidage is produced, often on distinct shear planes with tertiary creep sometimes occurring at strains of about 10% following the severe breakup of the structure. At low stresses, glass-ceramic (i) did not fail at all but merely continued to deform to strains well in excess of 40% (Fig. 4c) with no void generation.

For both glass-ceramics in both tension and compression, increasing strain to failure was obtained for decreasing stress but there was no definite trend for change of temperature within the range in which tests were made. In Fig. 5a and b the variation with stress is illustrated for glass-ceramics (i) and (ii) respectively. Each plotted point represents the average strain to the onset of tertiary creep for each stress level used, this also being found experimentally to be the point at which surface cracks appeared in tension. Creep rupture is discussed later.

Primary creep was subject to some scatter between specimens owing mainly to slight microstructural differences and, more especially in compression tests, to non-axialities of loading during bedding down onto the alumina pushrods. Although minimized experimentally, these factors caused considerable scatter since the total strain involved was small, generally less than 0.3%. In all cases, the total creep strain to a steady secondary creep rate increased with increasing stress as might be expected but remained effectively constant with changing temperature. An analysis of the primary creep and creep recovery of both glass-ceramics in compression will be reported in Part 2 of this work.

The general behaviour of the materials correlates well with the results of Lyall [2] for both tension and compression. Perhaps the most important feature of this behaviour is the very much greater stress required in compression than in tension to maintain the same creep rate. As Lyall pointed out, this is indicative of a dominant deformation process which is sensitive to the sign of the mean internal hydrostatic pressure or to the state of packing of the crystalline material. To investigate this process, it is necessary to analyse the secondary creep data.

4. Secondary creep

In general, the strain-rate $\dot{\epsilon}$ produced by an applied stress σ is the sum of the contributions made by each deformation process. Usually, only one deformation process is dominant and rate-controlling, and instead of a summation, the strain-rate can be written as:

$$\dot{\epsilon} = A(\sigma, T, s) \exp \left\{ - \frac{\Delta H(\sigma, T, s)}{RT} \right\} \quad (1)$$

where A and ΔH are effective functions describing the creep behaviour and where R is the gas constant, T is the temperature and s is a structure-related variable such as overall strain.

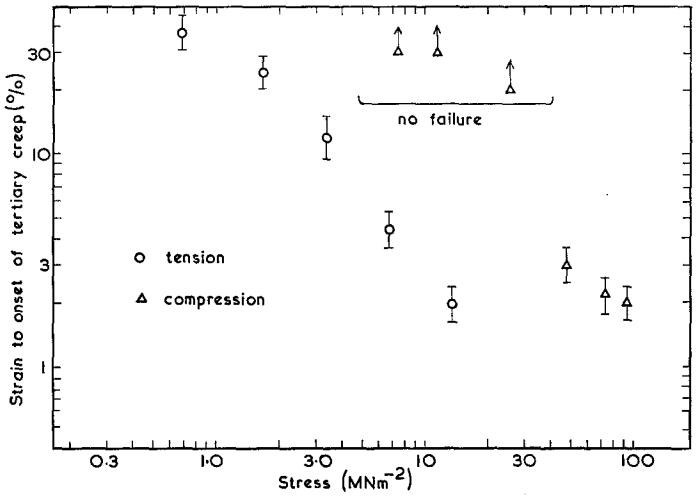

(a)

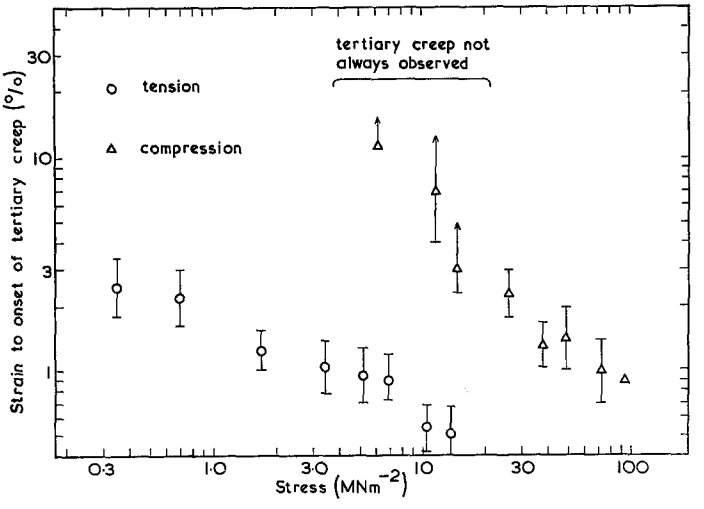

(b)

Figure 5 Variation of strain to the onset of tertiary creep with stress for (a) glass-ceramic (i), (b) glass-ceramic (ii).

Except at the highest stress levels used, the present experiments are characterized by a distinct secondary creep range up to the onset of failure, so s can be assumed to be effectively constant. Evaluation of A and H from the creep data relies on the ability to separate some of the variables of Equation 1, but generally, plots of $\{\log \dot{\epsilon}\}$ versus $\{1/RT\}$ and $\{\log \dot{\epsilon}\}$ versus $\{\log \sigma\}$ are made to provide an initial diagnosis.

In order to eliminate structural differences between specimens, stress or temperature changes should be made on individual specimens during secondary creep. However, the experimental methods used in this research required creep strain increments of about 0.1% for temperature changes and 0.2% for stress changes (owing to additional delayed elastic effects) in order to measure the strain-rate accurately for each set of conditions. Since the total strain to fracture was often low, less than 2% and in some tests as low as 0.2%, only a limited number of stress or temperature changes could be made on a given specimen. In many cases, a large number of individual tests had to be made and this incurred a greater scatter of results. The majority of creep tests were performed on glass-ceramic (ii) and, after establishing its general characteristics, a number of tests

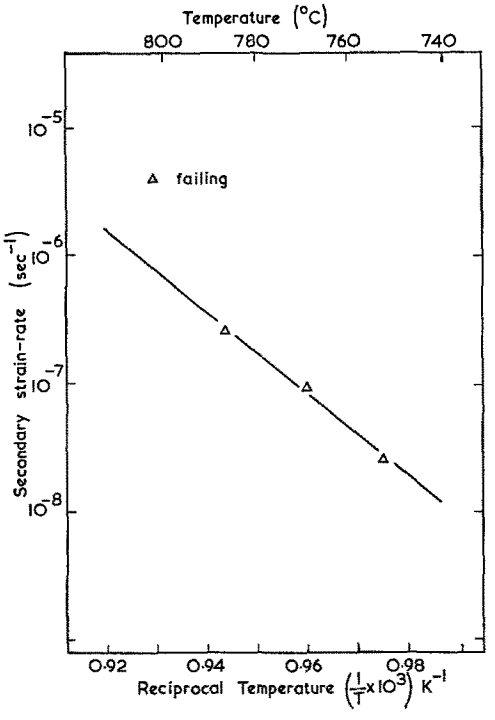

Figure 6 Arrhenius plot of a temperature change tension test on glass-ceramic (ii) at 0.69 MN m^{-2}.

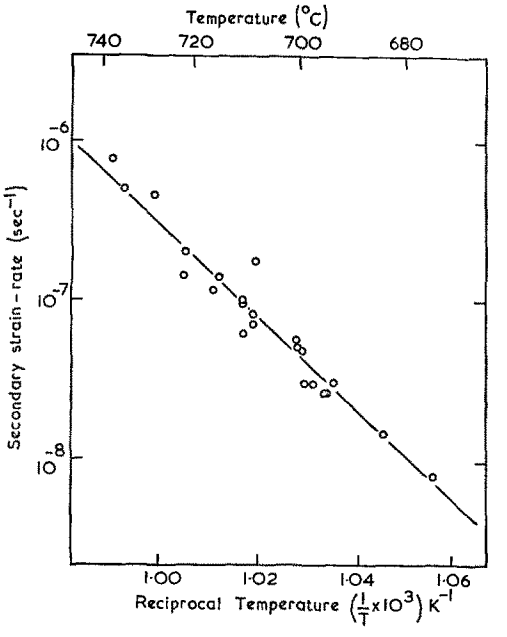

Figure 7 Arrhenius plot of a number of tension tests at 5.16 MN m^{-2} at various temperatures on glass-ceramic (ii).

were made on glass-ceramic (i) to ascertain similarities.

4.1. Glass-ceramic (ii)

4.1.1. Tensile tests

Fig. 6 summarizes the results of a temperature change test at 0.69 MN m^{-2}. The total strain to fracture was 2.25% of which 1.8% was in secondary creep, failure following shortly after the third change. The activation energy measured from the slope of the Arrhenius plot is 594 kJ mol^{-1}. At stress levels above about 5 MN m^{-2} this technique could not be used owing to the low fracture strain. Fig. 7 shows a similar plot of data from a large number of individual tests at 5.16 MN m^{-2}. Outside the scatter of the data there is no significant deviation from a straight line, the slope of which yields an activation energy of 560 kJ mol^{-1} calculated by a least squares method.

The results of all tests are summarized in Fig. 8 which shows the least squares fitted lines to data obtained at each stress level. For clarity the individual data are omitted, but the error bars represent the scatter about the fitted lines. The increasing size of error bars with increasing stress reflects an increasing sensitivity of the measured strain-rate to slight variations of specimen microstructure and alignment. Tests at 13.8 MN m^{-2} showed a minimum rather than a distinct secondary creep rate.

Fig. 8 demonstrates that the activation energy is effectively independent of stress within the test range, with an average value of 570 $\pm$ 40 kJ mol^{-1}. Thus, in Equation 1, the stress and temperature functions are separable, the pre-exponential A being a function of stress only. If this function is of the form $B\sigma^n$, then the stress exponent n can be established from the slope of a $\{\log \dot{\epsilon}\}$ versus $\{\log \sigma\}$ plot.

The data from a stress-change test are presented in this form in Fig. 9, and the stress exponent calculated from the slope of the least squares fitted line is 2.47. At higher stresses, stress changes on individual specimens are again precluded by strain limitations, so the form of the stress function is obtained from the least squares data plotted in Fig. 8 by correcting them to a common temperature. Fig. 10 shows a temperature compensated plot where the data has been corrected to 700°C by plotting

$$\log \left\{ \dot{\epsilon} \exp \frac{\Delta H}{R} \left(\frac{1}{T} - \frac{1}{973} \right) \right\} \text{ versus } \log \sigma .$$

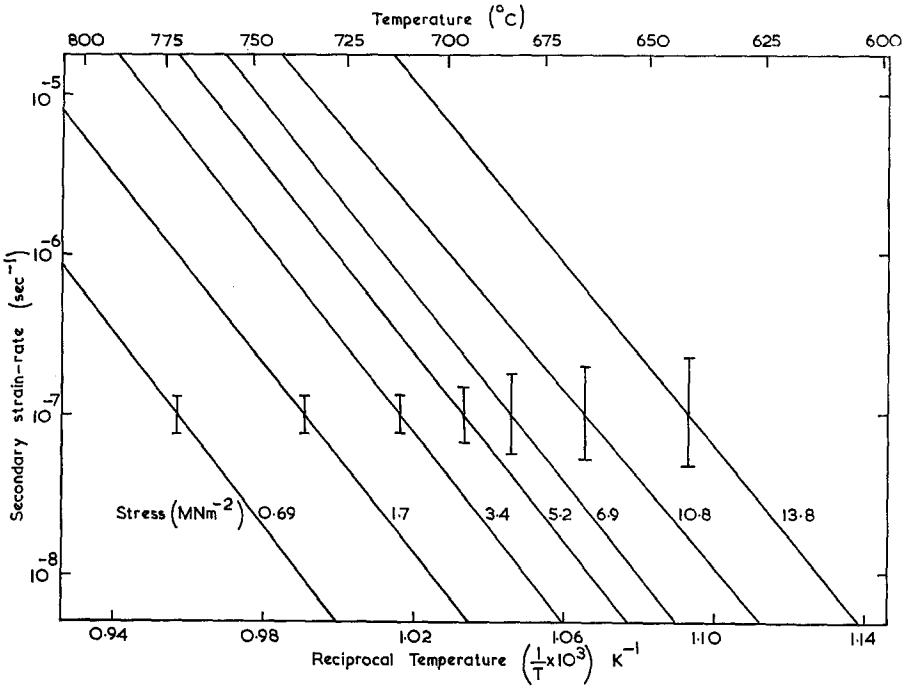

Figure 8 Arrhenius plot of the least squares fitted lines to data from all tension tests at different stress levels for glass-ceramic (ii). The error bars denote the scatter of the original data about the lines.

Tests at 13.8 MN m^{-2}, which showed only a minimum creep rate before failure, probably exaggerate the true secondary strain-rate and hence the true stress exponents. Nevertheless, the stress exponent evidently varies considerably in the stress range used and at no point was Newtonian creep (i.e. $n = 1$) observed.

4.1.2. Compression tests

Similar data to the tensile case were derived from compression tests, and were plotted in the same manner. Fig. 11 shows the least squares fit lines to the data of a large number of tests. The results are similar to the tensile case, Fig. 8, in that the activation energies were effectively independent of stress with a mean value of 610 ± 40 kJ mol^{-1}.

The corresponding temperature compensated plot for compression obtained by replotting the data of Fig. 11 shows a distinct upward curvature and is reproduced in Fig. 10 for comparison with the tensile case. The stress exponent again varies between 2.2 and 5.0 within the range of stress that produces distinct secondary creep.

4.1.3. Discussion

The most interesting feature of the secondary creep of glass-ceramic (ii) is the large variation of stress exponent with stress. This is a real effect,

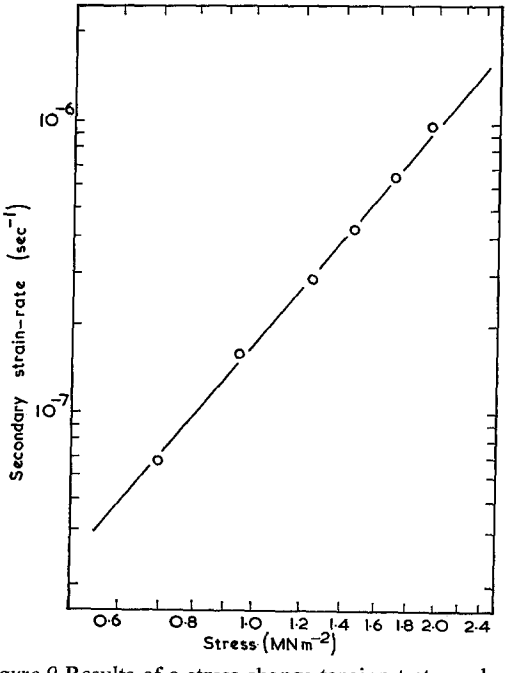

Figure 9 Results of a stress change tension test on glass-ceramic (ii) at 759°C.

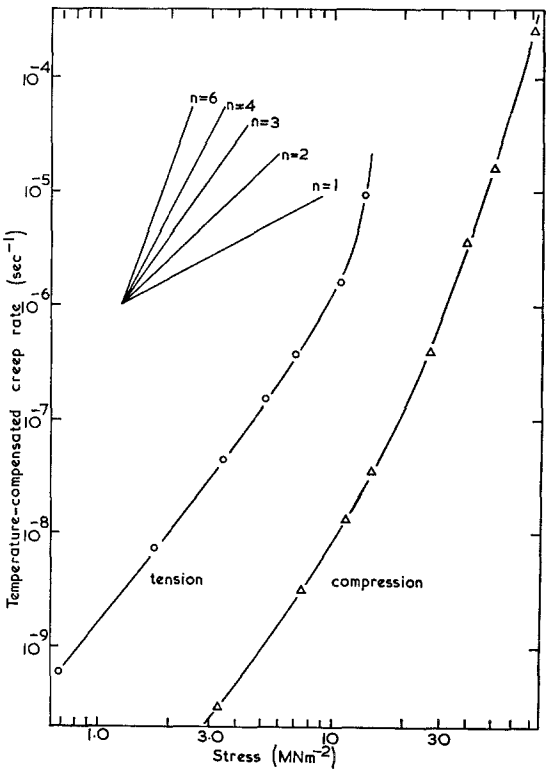

Figure 10 Temperature compensated creep plot for tension and compression on glass-ceramic (ii), derived from the least squares fitted data of Fig. 8 corrected to 700° C.

and not a consequence of the choice of the stress function σ^n, since no other simple function of stress produced a direct relation with strain-rate. The two sets of data in Fig. 10 produce curves of similar shape in tension and compression, the latter being displaced to a higher stress relative to the former. In neither case does the stress exponent equal unity, although the trends shown suggest that at stresses well below the capabiity of the testing machines, Newtonian viscous creep may occur. On the other hand the activation energies are approximately the same in tension and compression, and do not vary significantly with stress or temperature. This implies that the same thermally activated process controls the deformation at all stress levels, although at first sight the high stress exponents seem to rule out viscous flow of the residual glass phase.

The microstructure of glass-ceramic (ii) appears to be unchanged by tensile or compressive strains. There is no change in the volume fractions of the individual phases, nor of the crystal morphology and there is no evidence of a deformation texture. Fiducial lines on the polished surface of some tensile specimens demonstrated some relative movement of the lithium disilicate clusters but thermal etching impeded any detailed study. Similar results were obtained from a number of compression specimens with the surface crystallization layer removed. Samples tested in compression after 1 or 2% strain in tension underwent more primary creep strain than, but possessed the same secondary creep rate and net failure strain as an as-crystallized, previously unstrained sample tested in compression only at the same stress and temperature. Thus, tensile straining does not radically alter the structure of the material with respect to a compressive stress and failure of the material is determined by the net plastic strain and its sign only. To investigate the effects of crystal morphology on the deformation and failure processes, samples of glass-ceramic (i) were subsequently tested.

4.2. Secondary creep of glass-ceramic (i)

Glass-ceramic (i) was tested over the same range of stress and temperature as glass-ceramic (ii), but as the former possesses rather greater plasticity, stress and temperature change tests could be used over the greater part of the testing range, and fewer specimens were required to ascertain the creep behaviour.

Figs. 12 and 13 show the Arrhenius plots of all data for the tensile and compressive cases respectively. As with glass-ceramic (ii) the activation energy is effectively independent of stress and temperature within the testing range, with average values of 590 ± 30 kJ mol^{-1} in tension and 600 ± 40 kJ mol^{-1} in compression.

The corresponding temperature-compensated plots, Fig. 14, yield an average stress exponent of 1.9 for tensile tests with no significant variation with stress. In compression, however, there is a sharp transition from $n \approx 1$ at low stresses to $n \approx 4$ at stresses greater than about 26 MN m^{-2}. This distinct difference in behaviour correlates well with the transition from the situation of no failure at strains of less than 30% found at low stresses to one of low strain shear failure with the generation of local porosity at high stresses illustrated in Fig. 5. The individual stress change tests covering the range 3.4 to 30 MN m^{-2} verify this transition.

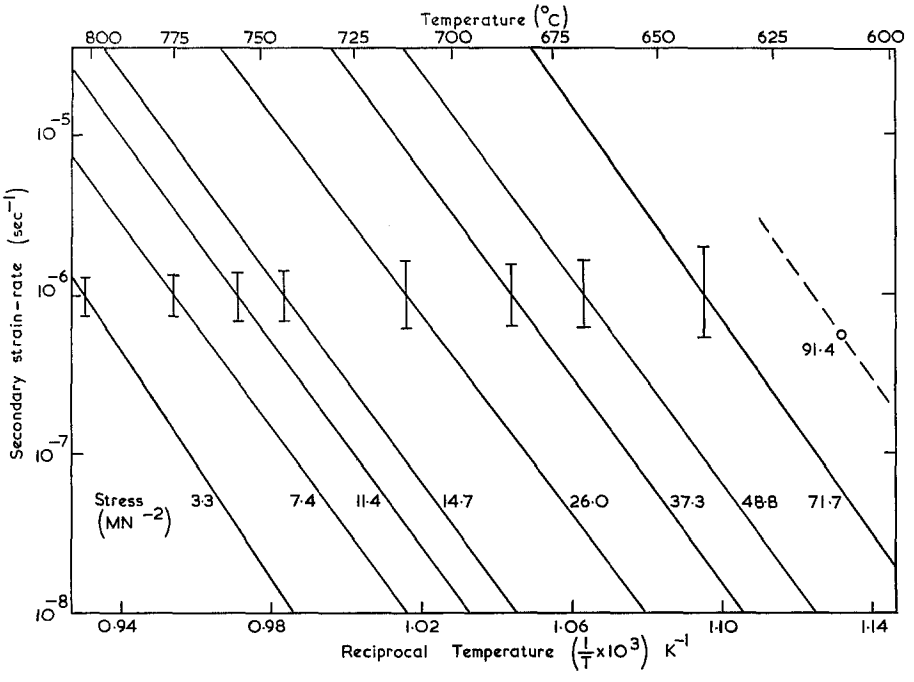

Figure 11 Arrhenius plot of the data from all compression tests on glass-ceramic (ii). The error bars represent the scatter of data about the least squares fitted lines to all data.

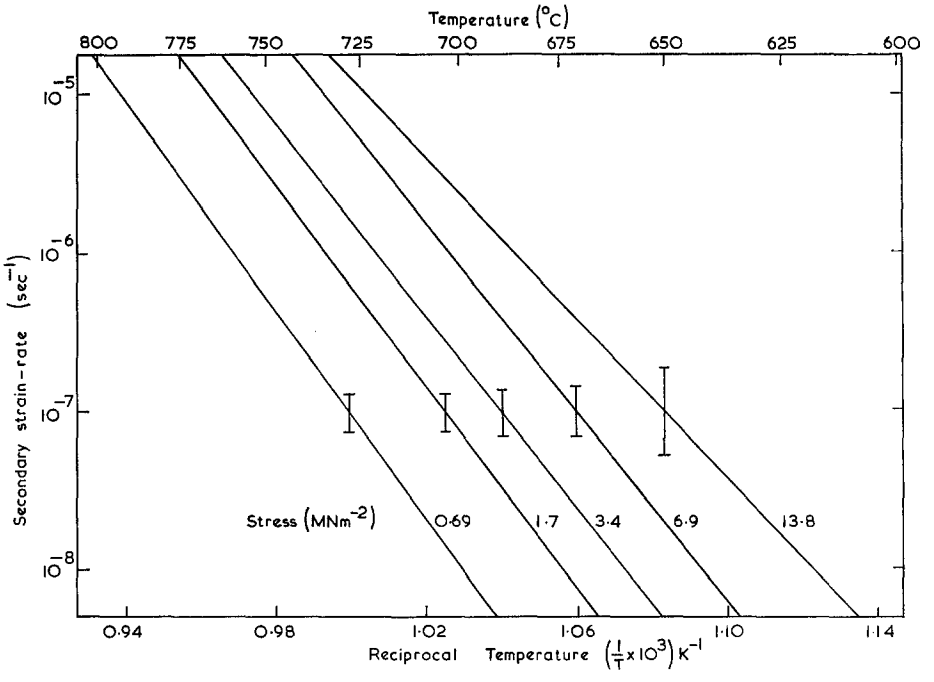

Figure 12 Arrhenius plot of the data from all tension tests on glass-ceramic (i).

4.2.1. Comparison of behaviour of glass-ceramics (i) and (ii)

The behaviour of the two glass-ceramics is similar in many respects. In both materials there is a considerable difference between the stresses required in tension and compression to maintain

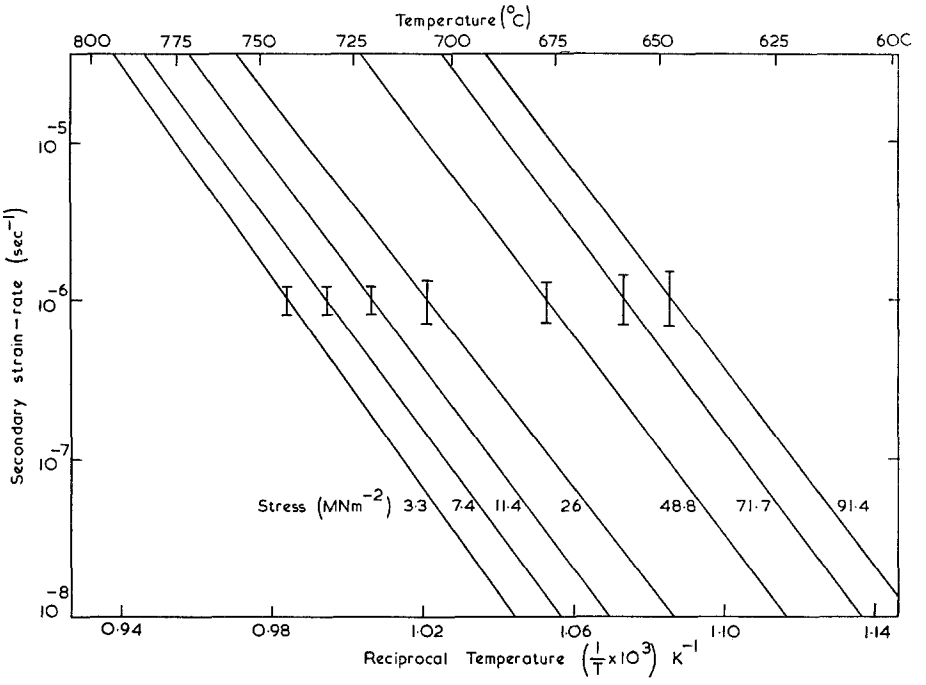

Figure 13 Arrhenius plot of the data from all compression tests on glass-ceramic (i).

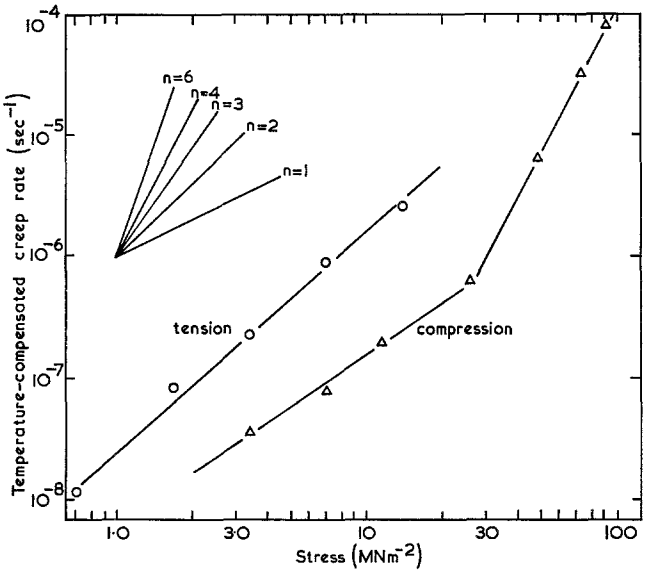

Figure 14 Temperature compensated creep plot for tension and compression on glass-ceramic (i).

the same creep rate, the activation energies are similar in tension and compression, and both materials suffer from low strain failure at high stresses. However, unlike glass-ceramic (ii), glass-ceramic (i) shows distinct Newtonian creep behaviour ($n = 1$) at low compressive stresses, at the same time exhibiting no tendency to fail in shear. Fig. 15 illustrates the microstructure developed in glass-ceramic (i) at high tensile and compressive strains by low stresses. There is evidence in the etch pattern that some grain re-orientation has occurred, compared to an as-

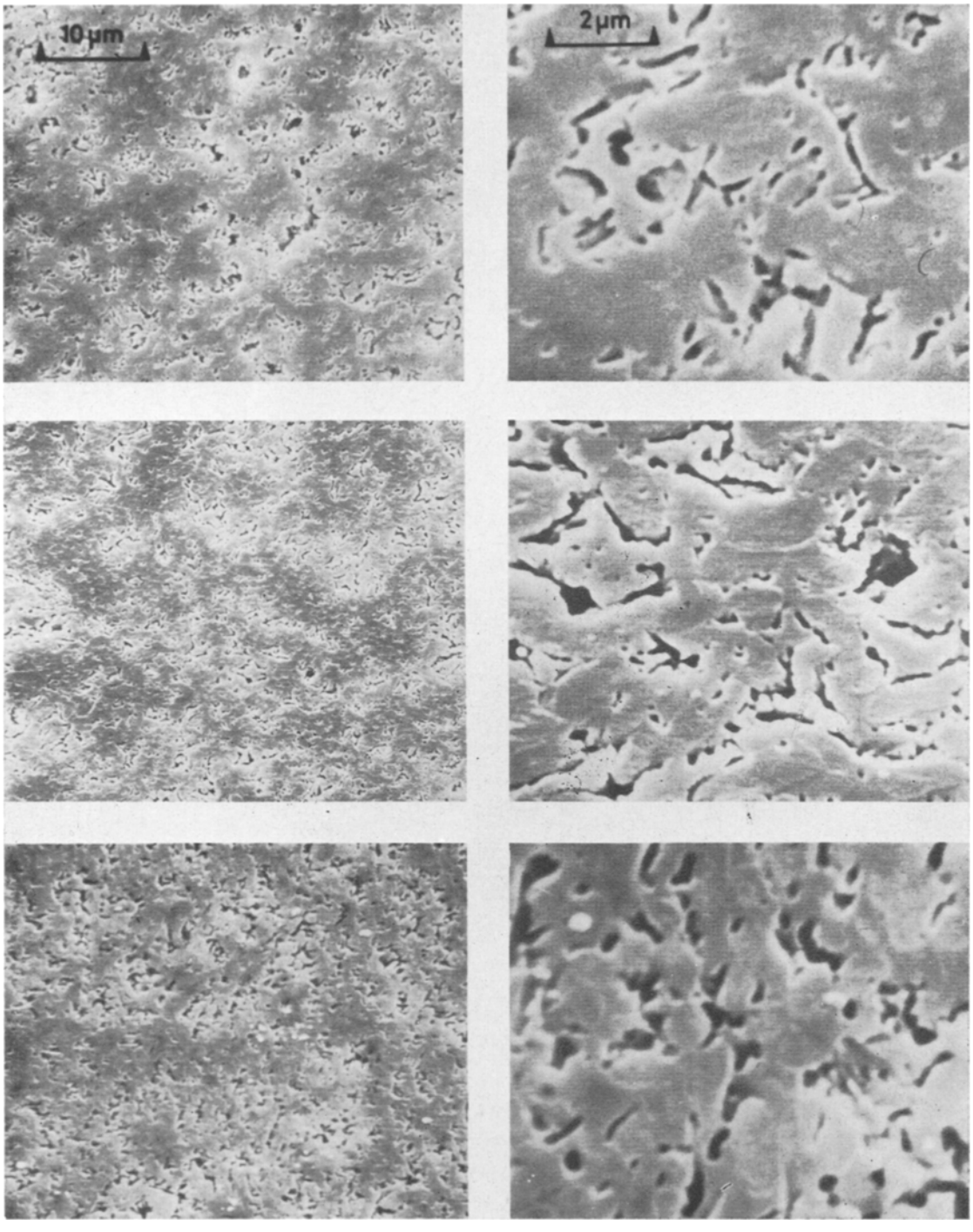

Figure 15 The microstructure of glass-ceramic (i) after (a) 25% tensile strain, (b) control, (c) 30% compressive strain at 780° C and at low stresses.

crystallized control sample, but no preferred orientation is evident in X-ray texture patterns and there is no change in the volume fractions of the phases by area analysis. The behaviour of glass-ceramic (i) at low compressive stresses can therefore be attributed to viscous creep of a solid-

liquid aggregate, but its behaviour at high compressive stresses ($n \sim 4$) and in tension at all stress levels ($n \sim 2$) does not fit this interpretation. Glass-ceramic (ii) does not exhibit Newtonian flow at any stress level.

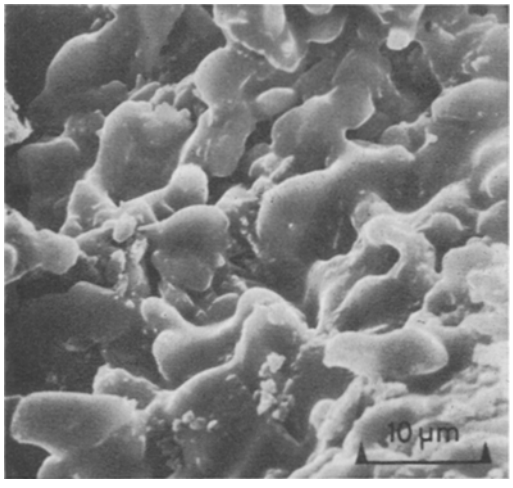

Figure 16 Fracture surface of glass-ceramic (ii) at 700° C, 1.7 MN m^{-2}.

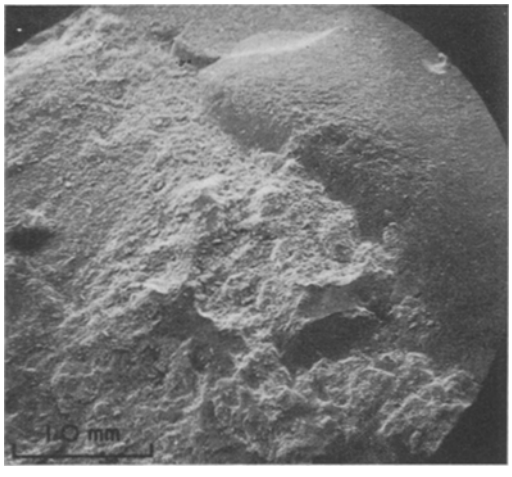

Figure 17 Fracture surface of glass-ceramic (i) at 600° C, 13.8 MN m^{-2}.

5. Creep rupture

As mentioned in Section 3, tensile creep specimens fail by the propagation of blunt cracks, generally from the surface. The fracture faces are very rough and have the appearance of crystals covered with a rounded layer of glassy material (Fig. 16). Bifurcation of the crack often occurs as a result of the inhomogeneous structure and at high stresses the fracture surface shows a region of brittle failure, typically as in Fig. 17. Examination of polished axial sections of failing specimens of both glass-ceramics reveals that the fracture path is usually confined to the glass phase between crystals in glass-ceramic. Fig. 18 shows a cross-section of a specimen of glass-ceramic (i) tested at low stress, 0.69 MN m^{-2}. Etching the surface has accentuated the width of many internal cracks which were generated perpendicular to the stress axis towards the end of secondary creep.

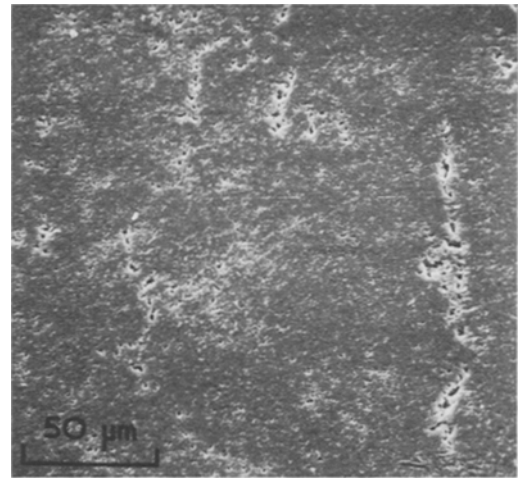

Figure 18 Polished and etched cross-section of a failing tension specimen of glass-ceramic (i) showing internal cracks. Stress axis horizontal.

In compression, failure occurs by the three modes illustrated by Fig. 4. At low stresses in glass-ceramic (ii), large scale porosity (Fig. 19a) results at strains greater than 5% although the specimen remains in one piece. The vast majority of voids appear to be closed and to have fairly smooth surfaces, sizes varying from about 5 μm up to 50 μm but generally smaller than the pre-existing porosity in this material. At higher stresses (Fig. 19b), shear failure is initiated by structural break-up, voids having been produced within both the glassy phase and the lithium disilicate clusters. This type of localized failure in a shear band may be initiated at low strains by groups of large pre-existing voids, and demonstrates that the shear strength of this type of structure is low.

High stress compressive failure of glass-

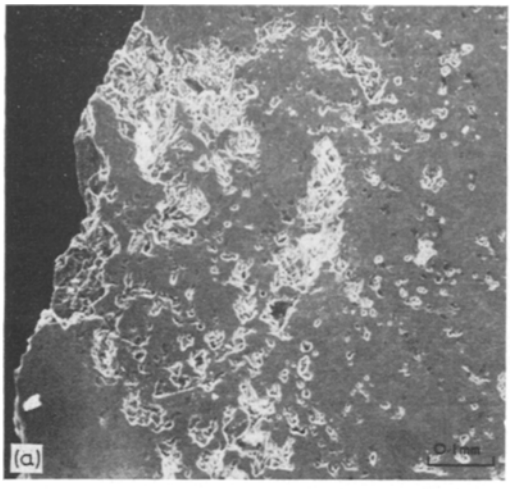

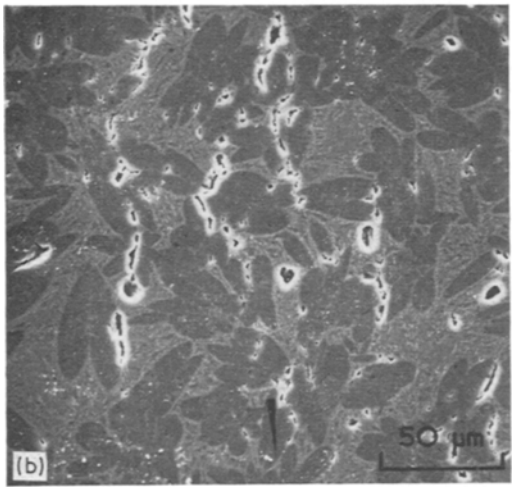

Figure 19 Porosity developed at compression failure in glass-ceramic (ii), (a) at low stress, (b) at high stress in the shear band before failure. Stress axis vertical.

ceramic (i) occurs in a manner similar to that exhibited by glass-ceramic (ii) except that the voided shear band is narrow, usually less than 50 μm thick, and the voids produced are extremely small. The subsequent sliding of the two halves of the specimen results in the tearing from the shear band of fragments 20 to 100 μm across, thus giving exposed sheared surfaces a powdery appearance.

It is concluded that in compression at least, creep rupture is caused primarily by the formation of voids between crystals and mainly within the glassy phase. These voids could arise only as a result of a locally negative hydrostatic pressure in the glass phase even under high compressive stresses, and their presence implies that there is insufficient percolation of fluid material between the solid particles to fill the increased interparticle volume arising from relative particle movement.

As pointed out earlier, there is a distinct correlation between the variations with stress of stress exponent and failure strain. Since void formation appears to be the primary cause of failure, the nucleation and early stages of growth of voids must occur during secondary creep. To investigate this possibility, creep specimens were quenched under load after various tensile and compressive secondary creep strains, and polished sections were examined in the scanning electron microscope. Fig. 20 illustrates that in both

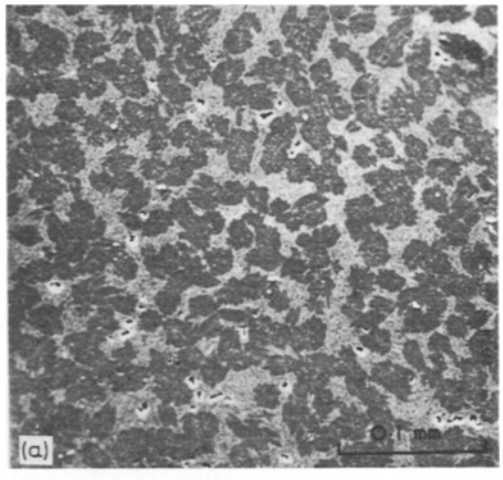

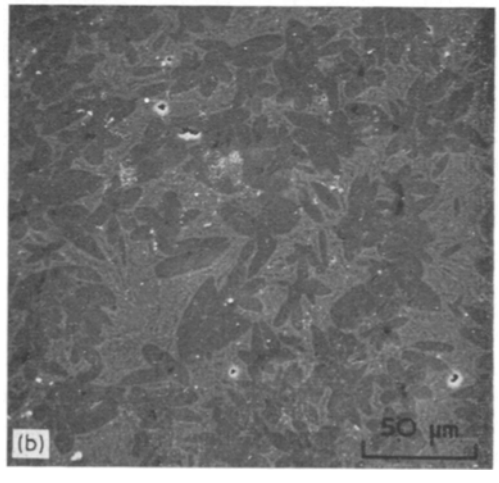

Figure 20 Voids produced prior to tertiary creep, (a) in tension, (b) in compression in glass-ceramic (ii). Stress axis vertical.

tension and compression, numerous small voids have been created in glass-ceramic (ii) during plastic strains of less than 1% and before the detection of any tertiary creep. Similar voids but on an extremely small scale were found in glass-ceramic (i). The fact that there are many more voids in tension than in compression is an obvious consequence of an average negative hydrostatic pressure within the tension specimen. In compression the average pressure is positive so that, in general, voids cannot be produced unless the geometry of solid material enclosing regions of fluid material is such that small local shear strains result in a net negative local pressure. The number of sites under these conditions is, therefore, likely to be very much smaller than under an equal tensile stress.

In specimens that were not quenched under load but which were allowed to recover somewhat before cooling from the test temperature, no conclusive evidence of void formation of this type was found. Few voids less than 5 μm across were found in failed specimens under the same conditions. Since small voids in fluids are mechanically stable only under a sustained negative pressure this is to be expected, the small re-arrangements taking place during creep recovery probably being sufficient to allow most small voids to close up.

6. General discussion

The facts that rapid creep rates are obtained at low stresses, that except for void formation within the glass phase there is no significant change in microstructure after testing, and that cracks are confined to the glassy boundaries between crystals suggest that the crystalline material is only weakly connected by the residual glass phase. This is borne out by the micrographs in Figs. 1 and 2. Consequently it is likely that the glass phase rate-controls the creep process. However, although the creep behaviour is characterized by a single activation energy for all stresses and temperatures, it is not Newtonian as might be expected. The experimental results indicate that a stress exponent of 1 is obtained only for glass-ceramic (i) at low stress. Under all other stress conditions in both materials, it is markedly greater than 1 and can be as high as 6, it increases with increasing stress and correlates with decreasing strain to failure and the occurrence of void formation. Since voids are the origin of specimen collapse in compression, their existence during secondary creep must have an effect upon the creep rate. The consequences of this phenomenon are now discussed by considering the glass-ceramics as rigid solid–liquid aggregates.

With volume fractions of fluid material of only about 20%, the aggregates might be expected to exhibit dilatancy in a manner analogous to wet sand, particularly so in the case of the large irregular interlocking crystals of glass-ceramic (ii) than to the more uniform structure of glass-ceramic (i). The characteristics of dilatancy have been reviewed by Frank [6]. The overall creep rate will depend on the rate at which the fluid material can percolate through the aggregate to relieve pressure gradients resulting from the dilatancy of the solid particles, thereby allowing inhomogeneous shear of one particle past its neighbour.

In a fairly close-packed aggregate, this inhomogeneous shear proces requires a reduction in the local packing density of the solid material, or an increase in the neighbouring interstitial fluid-occupied volume (e.g. wet sand dries temporarily when trodden upon as water is drawn in from the surface). This is accompanied by a reduction of the local interstitial pressure below the average pressure. The return of this pressure to normal, allowing a permanent particle displacement, can occur in either of two ways: (a) by percolation of fluid from regions at higher pressure, allowing deformation at constant volume, or (b) by the nucleation and growth of a void if a suitable nucleation site is available and if the local pressure is sufficiently negative for this to occur. Method (a) should occur generally throughout samples of both glass-ceramics, and the deformation rate resulting will be controlled by the viscous glass, assuming that structural changes within the crystalline material are negligible. On the other hand, the effectiveness of method (b) depends critically on several factors. These are principally: (1) the irregular distribution of solid material which, when stressed, gives rise to fluid regions under a locally negative hydrostatic pressure; (2) the void nucleation characteristics under negative pressure; (3) the effect of a void on the shear rate of the solid material around it resulting from the redistribution of shear stress.

After nucleation, occurring most probably at a glass-crystal interface, the opening of a void will be resisted only by the glass viscosity and surface tension. As a consequence the material surrounding a void can deform at a variable local volume,

a process which eases inhomogeneous shear deformation considerably since the relatively slow process of fluid percolation is no longer required. Since this small volume now has much less resistance to shear, the applied stress will have to be supported by neighbouring void-free regions which then either deform by method (a) at an increased rate, or produce further voids depending on the geometry of the solid material. Since void nucleation appears to occur readily, it is probable that most regions of high negative hydrostatic pressure are relieved soon after initial stressing. If subsequent deformation is by method (a) at an increased rate, then a steady creep rate (considerably faster than in the absence of voids) will occur up to a strain at which the alteration of the solid particle configuration causes further voids to be nucleated. The strain-rate then accelerates to failure. In compression, failure will occur when the distribution of voids is such as to produce a plane of weakness in shear whereas in tension internal cavitation will occur. However, tensile failure was observed to result mainly from blunt surface cracks which propagated at very low strains, internal cracks being found only at low stresses where the growth of surface cracks was much reduced. At all stages of this process, the glass phase controls the rate of deformation at every point within the materials. The activation energy of creep should, therefore, be the same as the viscous activation energy of the glass phase under all conditions, as is shown experimentally.

Where deformations greater than about 5% are involved, it is conceivable that two other phenomena could occur. Firstly, a shear hardening could arise as the solid particles become better packed in shear directions, but such compaction is seen in neither glass-ceramic, even up to strains of 30% for glass-ceramic (i). Indeed if void formation can occur in an aggregate then shear-hardening is unlikely to exist unless crystalline deformation or a change in the microstructure of the aggregate occurs. Secondly, it is possible that as the solid particle configuration changes with shear then, during fairly large local strains, the sign of the hydrostatic pressure could change and cause voids to close up again. With this model it would be possible to produce large deformations with non-Newtonian characteristics, as was shown by glass-ceramic (i) in tension with $n \approx 2$.

The exact form of the stress exponent cannot be calculated since the factors listed above defining the behaviour of the aggregate in the presence of a void preclude the use of simple mathematics, but an approximate form can be demonstrated as follows: The secondary creep is the product of that due to normal percolation of fluid and the stress concentration factor due to void formation and stress transfer. If in a given volume of solid-liquid aggregate there are x_0 glassy areas, then under an applied uniaxial stress σ, a number $x(\sigma)$ will have voids nucleated in them, neglecting time or strain dependence of nucleation. The stress supported by the material immediately surrounding each void will be transferred to neighbouring areas. If each such stress-relieved region contains y glassy areas, then assuming that its deformation resistance is negligible compared to its surroundings, the stress on the surroundings will be increased by the factor

$$x_0/\{x_0 - yx(\sigma)\}\,.$$

In a uniaxial test, the strain-rate $\dot{\epsilon} = \sigma/(3\eta^*)$, where η^* is the effective aggregate viscosity, becomes

$$\dot{\epsilon} = \frac{\sigma}{3\eta^*}\left\{\frac{x_0}{x_0 - yx(\sigma)}\right\}.$$

The stress exponent is, therefore,

$$n = \left(\frac{\partial \ln \dot{\epsilon}}{\partial \ln \sigma}\right)_T = 1 + \left\{\frac{\sigma \,.\, y}{x_0 - yx(\sigma)}\right\} \cdot \left(\frac{\partial x}{\partial \sigma}\right)_T .$$

The form of n is dependent on y and $x(\sigma)$ and hence on the microstructure, but is similar to that shown by the glass-ceramics, increasing rapidly with increasing stress.

In Fig. 20a, 40 voids were found in a total of about 200 possible sites. The stress exponent measured at that stress level was 4. If these values are put into Equation 2 with the assumption that $(\partial x/\partial\sigma) \approx (x/\sigma)$, then $y = 3.8$ and hence the number of nearest neighbour glassy regions affected by each void is 2.8. This would appear to be a reasonable figure for the interlocked structure of glass-ceramic (ii).

The experimental behaviour of the glass-ceramics can, therefore, be explained at least in qualitative terms by a mechanism allowing void formation within the residual glass phase, based on the assumptions that the material is in phase equilibrium and that the crystalline material does not deform enough to contribute significantly to the creep rate. In respect of the first assumption it should be noted that in order to equilibrate their structures, the glasses were heat-treated to a

temperature rather higher than the maximum used in creep testing, although not so high as to cause significant dissolution of crystalline material. It is unlikely that bulk crystal deformation controls the deformation since the microstructure contains mainly isolated crystals in a glassy matrix as opposed to small areas of glass in a more rigid crystalline matrix. Also, the structures deformed very rapidly at very low stresses in the temperature range in which the glass phase was fairly fluid, i.e. at stresses well below the expected creep strengths of the complex crystalline silicates. A more likely deformation process is local dissolution and sintering of crystalline material, with the glassy phase acting as a solvent through which matter transport takes place. In this case, the packing of crystalline material in the stress directions (axial and shear) would be improved in compression and worsened in tension as the number of points of high stress concentration are progressively eliminated. Strain-hardening would probably result especially in compression, and the stressed structure would not be in equilibrium. However, the glass-ceramics showed a steady creep rate after a reproducible primary creep and no shear-hardening even up to strains as high as 30% in compression in glass-ceramic (i). Further, it is difficult to visualize how compression shear failure might be a consequence of such a mechanism.

Thus, while the existence of changes in the crystal morphology during creep cannot be eliminated, especially as the mechanical properties of the crystalline material are essentially unknown, it is felt that such changes do not control the creep rate of the glass-ceramics. The experimental evidence presented here suggests that the glass phase, coupled with the general crystal morphology, is responsible for the observed creep and fracture behaviour.

7. The creep rate controlling processes in refractory ceramic products

A variable stress exponent has also been found in a number of widely differing refractory ceramic products. For example, Clews *et al* [7] studied several porous refractory products and on making due allowance for shrinkage and strain-hardening owing to their not possessing equilibrium structures, found that the stress exponent for creep is generally greater than 1. For example, an insulating firebrick in compression gave $n = 4$, while a fire clay produced a value between 2 and 4 increasing with increasing stress, but apparently independent of the initial porosity (between 30 and 60%). For a porcelain in tension n is about 2.5 but in compression n varies between 2 and 4 as in the fire clay. It was concluded that a molecular rather than macroscopic process controls the deformation. More recently, the data given by Hulse and Pask [8] can be used to calculate a stress exponent of about 4 for a dense fire clay refractory, while after allowing for phase changes in the specimens the activation energy was found to be 715 kJ mol^{-1}. The authors concluded that, whereas the amount of liquid phase affects the overall creep rate, it rate-controls the deformation only in the absence of a continuous network of mullite crystals.

Since the above materials contain a fairly high proportion of liquid phase they are similar in many respects to the glass-ceramics of the present paper. In the cases where deformation relies on the glass phase rather than on a continuous crystalline network, it is possible to apply the principle of void formation during creep to explain the high stress exponents obtained. In materials with considerable pre-existing porosity, the number of sites in which further voids can be nucleated is somewhat reduced compared to a dense material, but even so a stress exponent greater than 1 is expected.

It is concluded that the existence of glassy material in ceramic products in which the crystal network is neither continuous nor rigidly interlocked, leads to an enhanced creep rate and a low fracture strain due to the nucleation and growth of voids within the glass phase.

8. Conclusions

The creep properties of two lithium zinc silicate glass-ceramics of similar composition but very different morphology, each containing about 20% of residual glassy phase, are summarized as follows.

1. Compression creep requires between 3.5 and 7 times the stress in tension to maintain the same secondary creep rate.

2. In both tension and compression, increasing test stress produces a decreasing strain to failure.

3. The activation energy of secondary creep is effectively independent of stress and temperature within the range of the creep tests, and to within experimental scatter is the same in tension and

compression for both glass-ceramics – 600 ± 60 kJ mol^{-1}.

4. The stress exponent of secondary creep is independent of temperature but generally increases with increasing stress within the ranges 1.0 to 4.0 for glass-ceramic (i) and 2.2. to 6.0 for glass-ceramic (ii).

Examination of the microstructure of failing creep specimens showed that void formation occurs within the glassy phase, even in compression, indicating that regions of negative hydrostatic pressure exist as a consquence of the dilatancy of the relatively hard irregularly distributed crystalline material. Further, it was established that void formation occurs during secondary creep in both tension and compression, resulting in a faster creep rate than would have been produced in a similar void-free structure. A simple model has been applied to this complex behaviour and has demonstrated that a stress exponent varying with stress is to be expected although deformation is still controlled by the glass phase.

The existence of this phenomena is undesirable as it enhances creep rate and promotes low strain fracture, underlining the importance of promoting the growth of a continuous network or an interlocking structure of crystalline material in both glass-ceramics and refractory products.

Acknowledgements

The authors would like to thank Mr H. N. Young for technical assistance, Mr D. J. Clinton of the National Physical Laboratory for the transmission electron microscopy and Professor F. C. Frank, Dr J. S. Shah and Dr B. C. Masters for valuable discussion. The work was performed jointly at the Berkeley Nuclear Laboratories of the CEGB and Bristol University, under a Co-operative Award in Pure Science from the SRC for R. Morrell.

References

1. P. W. MCMILLAN, "Glass Ceramics" (Academic Press, London and New York, 1964).
2. R. LYALL, Ph.D. Thesis, University of Bristol.
3. A. R. WEST and F. P. GLASSER, *J. Mater. Sci.* **5** (1970) 557.
4. J. P. POOLE, *J. Amer. Ceram. Soc.* **32** (1949) 230.
5. R. MORRELL, *J. Phys. E.* **5** (1972) 465.
6. F. C. FRANK, *Rev. Geophysics.* **3** (1965) 485.
7. F. H. CLEWS, H. M. RICHARDSON, and A. T. GREEN, *Trans. Brit. Ceram. Soc.* **43** (1944) 223; **45** (1946) 161, 255.
8. C. O. HULSE and J. A. PASK, *J. Amer. Ceram. Soc.* **49** (6) (1966) 312.

Received 25 January and accepted 9 April 1973.